# Heat-pulse rectification in carbon nanotube Y junctions

Eva Gonzalez Noya*
*Departamento de Química-Física, Facultad de Ciencias Químicas, Universidad Complutense de Madrid, E-28040 Madrid, Spain*

Deepak Srivastava†
*Advanced Aerospace Materials and Devices, NASA Ames Research Center, MS 229-1, Moffett Field, California 94035-1000, USA*

Madhu Menon‡
*Department of Physics and Astronomy and Center for Computational Sciences, University of Kentucky, Lexington, Kentucky 40506, USA*

(Received 25 July 2008; revised manuscript received 30 October 2008; published 24 March 2009)

Using molecular-dynamics simulations we demonstrate the existence of heat-pulse rectification in carbon nanotube Y junctions. The heat pulse is found to propagate unimpeded from stem to branches, while in the reverse direction there is a substantial reflection back into the branches with significantly reduced transmission. Based on this we discuss the implications for phonon rectification applications for these junctions.

DOI: 10.1103/PhysRevB.79.115432 PACS number(s): 61.46.Np, 61.48.De, 68.65.−k, 81.05.Tp

## I. INTRODUCTION

Any useful transport applications of new generation of novel molecular materials require controllable anisotropic conducting behavior. Multiterminal junctions of carbon nanotubes (CNTs) constitute one such material with tremendous potential. Electronic current rectification in CNT Y junctions has been demonstrated both experimentally[1,2] and theoretically.[3,4] The rectification was shown to be a consequence of symmetry and chirality of the CNTs forming the "stems" and "branches" of the Y junctions.[4] The possibility of transmission, reflection, and rectification of collective mechanical vibrational waves or phonons in nanotubes or nanotube-based materials could similarly give rise to next generation of devices for miniaturized thermal, infrared, and radio-wave applications. For example, very recently experimentalists have reported a breakthrough in controlling field emission in nanotubes by a selective transmission of radio waves.[5] As a result, the key functions of a radio have now been radically miniaturized using the mechanical vibration of a single carbon nanotube. Furthermore, by adjusting the length of the nanotube, they were able to control the frequency of the radio signal that could be received. Using heat-pulse propagation through carbon nanotube Y junctions, we show that rectification of selective mechanical vibrational waves is possible in these nanoscale material structures. Hence, these could be used for selective phonon or mechanical vibration filtration or transport application.

For thermal transport, under steady state, it is well known that CNTs exhibit very large axial thermal conductivity.[6–8] It should be noted, however, that vibrational phonon modes play dominant roles, both in steady state as well as in transient thermal transport processes. These modes could individually very well depend strongly on the presence of defects in the underlying graphene lattice structure.[8] In view of the rectification and switching behavior seen in the electrical transport through branched CNT junctions, a study of the propagation of phonons or thermal pulses through branched CNT junctions is of great interest since it may lead to thermal switching or logic devices of technological importance. This could have useful applications in selective phonon transport and filtering for energy storage and reducing thermal noise in quantum computing. Interestingly, an experimental observation of thermal rectification in mass-loaded carbon and boron nitride nanotubes has very recently reported.[9] Theoretical works using nonequilibrium molecular dynamics (MD) have shown the existence of thermal rectification in straight CNT junctions[10] as well as in carbon nanohorns.[11]

In this work we report on MD simulations of heat-pulse transport in a branched CNT Y junction. Such junctions have been synthesized in template-based chemical vapor deposition (CVD) in a controlled manner.[1] The junction chosen consists of a zigzag (14,0) stem branching into two zigzag (7,0) tubes. Here we have used the chiral notation for nanotubes.[12]

## II. COMPUTATIONAL DETAILS

The MD simulations are performed using the Brenner bond order potential which has been shown to describe the thermal properties in carbon systems well.[13] The lengths of the stem and of the branches of the CNT Y junction are chosen sufficiently large enough to monitor a clear transport of the heat pulse through the junction. The Y junction consisted of 11 092 atoms with a total length of 843.48 Å. The Y junction is partitioned into a number of slabs with each slab consisting of two CNT unit cells and within each slab the instantaneous kinetic temperature is calculated and averaged over 50 time steps (25 fs) (Ref. 14) to allow a clear heat-pulse transport signal through the junction. Noise in the data is further reduced by averaging the results over four trajectories starting from different initial conditions. The equations of motion were solved using a fourth-order Gear predictor-corrector algorithm with a time step of 0.5 fs.[15] The initial conditions of the system are obtained by assigning random velocities, with a Gaussian distribution centered at 1 K, to the atoms located at their 0 K equilibrium positions and letting the system equilibrated for a few thousand MD steps.

 

During the simulations, the outermost slabs of each of the stems and branches of the junctions are held fixed and the heat pulses are applied on the atoms next to these slabs. The heat pulse is simulated by a three-step process: (1) during the first 0.1 ps, the temperature of the atoms in the five unit cells (heat bath) is increased to 800 K and followed by (2) free equilibration of the system during the next 0.8 ps followed by (3) the quenching of the heated atoms to 100 K during the last 0.1 ps. The heating and quenching in steps (1) and (3), respectively, were applied through a rescaling of the atomic velocities on these first slabs. The total duration of the application of the heat pulse is, thus, 1 ps and the heat-pulse transport in both the forward, i.e., from stem to branches, and reverse, i.e., from branches to the stem, is studied. The evolution of the system was then followed for more 4 ps, so that the total length of each simulation was 5 ps.

The amount of heat transmitted and reflected in each case was quantified by defining transmission, absorption, and reflection coefficients (denoted by $T$, $A$, and $R$, respectively) in the following way:

$$T = \frac{\text{Transmitted signal}}{\text{Incident signal}}, \quad A = \frac{\text{Absorbed signal}}{\text{Incident signal}}. \quad (1)$$

The reflection coefficient is obtained by using the principle of conservation of energy,

$$T + A + R = 1. \quad (2)$$

The incident and transmitted signals correspond to the kinetic energy of the leading heat pulse some time before and some time after crossing the junction, respectively. The absorption signal is the energy that remains in the junction some time after the heat pulse has crossed it.

## III. RESULTS

In this section we present our results for heat-pulse propagation in CNT Y junctions. Since the Y junctions are formed by the joining of three CNTs, chirality consideration lead to a large number of possible permutations. We, however, restrict our calculations to two symmetric Y junctions, namely, (14,0)-(7,0)-(7,0) and (10,10)-(5,5)-(5,5). The (14,0)-(7,0)-(7,0) Y junction (Fig. 1, left) consists of a (14,0) tube branching into two (7,0) tubes with an acute angle between them. This structure contains six heptagons clustered in the middle (shown in red) and no pentagons in an otherwise hexagonal arrangement of carbon atoms. The (10,10)-(5,5)-(5,5) Y junction (Fig. 1, right) also contains topological defects in the form of six heptagons and zero pentagons. However, some of these heptagonal defects extend into the branches.

The transient heat flow in the forward direction (stem to branches) for the CNT (14,0)-(7,0)-(7,0) Y junction is shown in Fig. 2. As seen in the figure, there is a clear passage of the heat pulse in the forward direction. The heat-pulse signal maintains its peak structure after crossing the junction and suffers only a slight loss in intensity with 67% of the incident signal crossing the junction and 25% of it being absorbed at the junction. As the color coding shows, no heat-pulse residue is left in the stem; i.e., there is very little reflection.

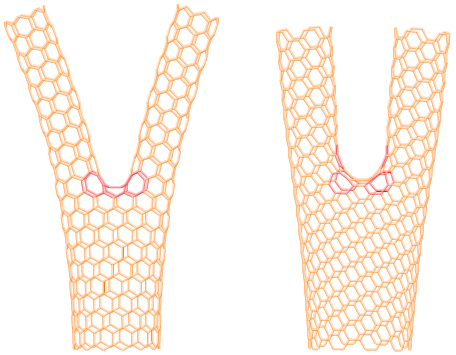

FIG. 1. (Color online) Carbon nanotube symmetric Y junctions consisting of (left) a zigzag (14,0) stem branching into two zigzag (7,0) tubes and (right) an armchair (10,10) stem branching into two armchair (5,5) tubes. The topological defect rings in the junction region consists of heptagons and shown in red (dark gray).

In the reverse direction (shown in Fig. 3), the heat pulse is originated at the branch ends and transmitted to the stem. The transmission coefficient drops to only 14% and about 40%–45% of the incident signal is either absorbed or reflected at the junction. The color coding clearly shows the residual heat pulse, i.e., substantial reflection back in the branches. These results show the existence of an anisotropy in pulsed thermal transport across a symmetric CNT Y junction similar to that found typically in the electronic transport devices based on CNT Y junctions.[3] Figure 4 (top and bottom panels) quantifies the main results obtained for the transient heat-pulse transport or propagation along the (14,0)-(7,0)-(7,0) Y junction. The absorbed signal was calculated as the integral of the instantaneous kinetic-energy curve between 100 and 300 Å at $t=1$ ps (see upper panel). The transmitted signal was estimated as the sum of areas under the two branch curves between 600 and 800 Å at $t=3.5$ ps and the absorbed signal was estimated as the area under the region of the junction (estimated to be the region between 350 and 450 Å) at $t=3.5$ ps. Note that, while the definition

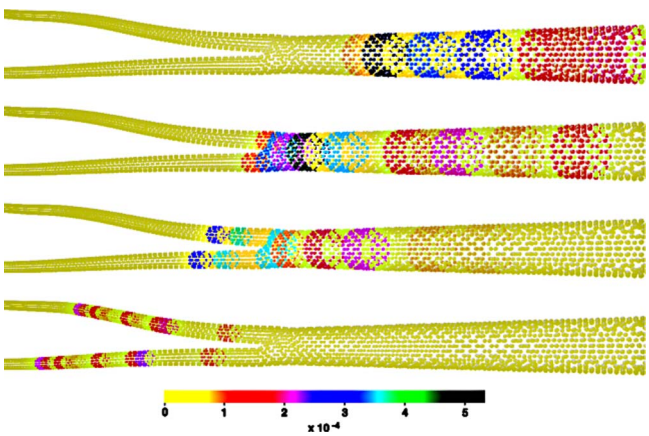


FIG. 2. (Color online) Heat-pulse propagation along the (14,0)-(7,0)-(7,0) Y junction in the forward direction (from stem to branches). The color coding shows kinetic temperature in arbitrary units. The heat pulse passes through the junction with some dissipation at the junction region and with very little reflection.

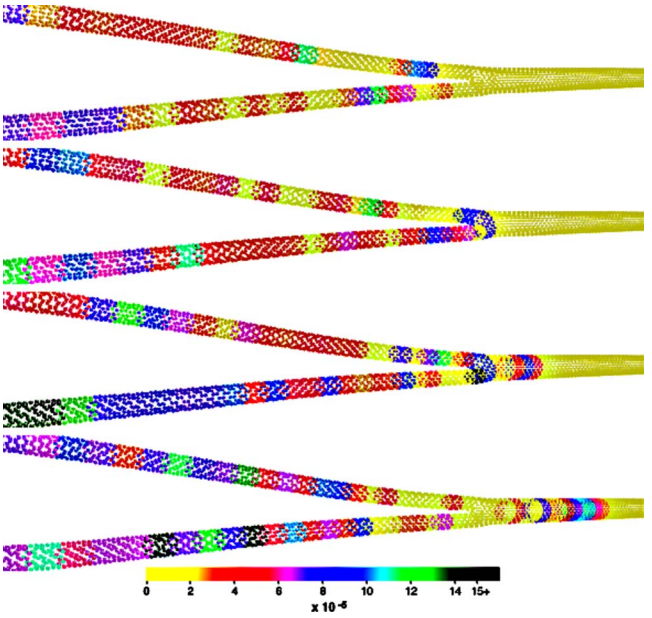


FIG. 3. (Color online) Heat-pulse propagation along the (14,0)-(7,0)-(7,0) Y junction in the reverse direction. The color coding shows kinetic temperature in arbitrary units. There is substantial reflection at the junction.

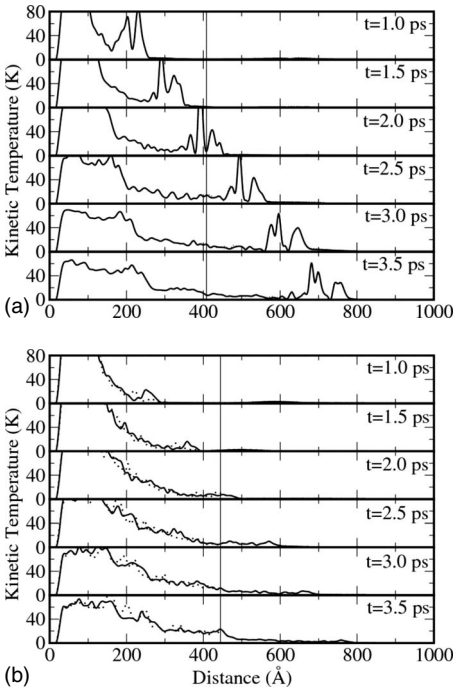


FIG. 4. Heat-pulse propagation along the (14,0)-(7,0)-(7,0) Y junction in the forward (top panel) and reverse (bottom panel) directions. A solid and two dotted lines are used to show the behavior of the two branches. The vertical lines mark the junction position.

of coefficients $T$, $A$, and $R$ is somewhat arbitrary, the focus of the present calculations is to investigate whether or not the heat is transmitted through the junction, rather than giving accurate estimates of the heat passage. As can be seen in Fig. 4 (top), as well as in Fig. 2, there is a clear passage of the heat pulse in the forward direction. Similarly, Fig. 4 (bottom) as in Fig. 3 shows reflection back in the branches.

The anisotropy found for the heat-pulse transport in the (14,0)-(7,0)-(7,0) Y junction case contrasts with recent results of thermal transport across Y junctions under steady-state conditions, which showed no anisotropy in the thermal conductivity across the (14,0)-(7,0)-(7,0) Y junction.[16] This is not surprising because the thermal transport under steady-state conditions, for thermal conductivity, can have long-time contributions from not only the leading phonon modes but also the contributions from the second-sound wave and the diffusive components. The diffusive thermal transport, dominated by multiple phonon-phonon scattering events, is not expected to be dependent on the nature of the junction and the underlying lattice structure. In the transient heat-pulse transport described here, the leading edge transport phenomenon is determined by the nature and propagation of discrete phonon modes and not overwhelmed by the long-time contributions from the diffusive components.

To test the validity of the above explanation, and to gather insight on the mechanism of anisotropic transient thermal transport across the zigzag (14,0)-(7,0)-(7,0) Y junction, the excited primary vibrational modes along the axial, radial, and azimuthal directions are investigated via the behavior of the corresponding vibrational amplitudes during the passage of the propagating heat pulse. To compute the time-dependent behavior of the radial and longitudinal mean-square vibrational amplitudes, defined as

$$\langle u_\alpha^2 \rangle = \frac{1}{2} \sum_{i=1}^{N} [\langle r_{i\alpha}^2 \rangle - \langle r_{i\alpha} \rangle^2], \tag{3}$$

where the subscript $\alpha$ stands for the radial or axial direction, one slab each in the stem, the junction, and in the two branches, consisting of five unit cells are monitored. $r_{i\alpha}$ are the radial and axial components of the atomic positions in a cylindrical coordinate system. The angular brackets denote time average. The vibrational amplitudes, time averaged over 40 steps (0.02 ps), are computed as the heat pulse traverses the monitored regions.

Figure 5 shows the variation of the axial mean-square vibrational amplitudes with time when the heat pulse is traveling along the (14,0)-(7,0)-(7,0) Y junctions. As seen in the figure, the longitudinal vibrational component of the wave packet in the forward direction suffers relatively very low reflection and some absorption and scattering at the junction. The transmitted component preserves the shape with a very small loss of magnitude. In the reverse direction, however, reflection, scattering, and absorption are very strong at the junction position. The transmitted component significantly loses both its shape and magnitude during the propagation through the junction. The time-dependent behavior of the axial vibrational amplitude, qualitatively representing the transport via axial vibrational modes, is therefore anisotropic in nature with a facile transmission in the forward and significant reflection and absorption in the reverse direction. The radial amplitudes show significant reflection and absorption at the junction equally in the forward and reverse directions, as shown in Fig. 6. The amplitude of the net transmit-

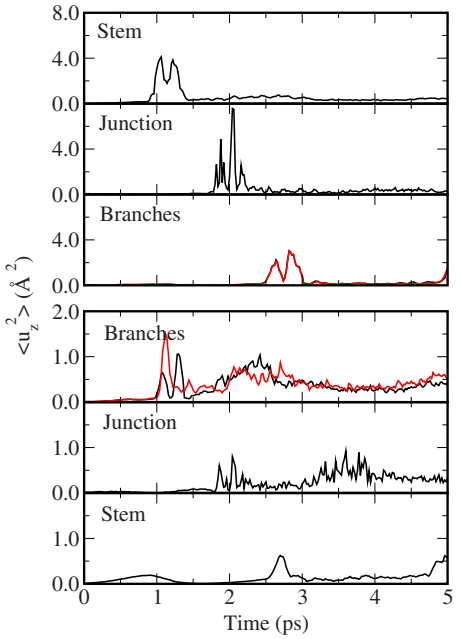


FIG. 5. (Color online) Time evolution of the longitudinal vibrational amplitude during a heat-pulse propagation in the (14,0)-(7,0)-(7,0) Y junction in the forward (upper panel) and backward (lower panel) directions. Black and red (dark gray) lines show the different behaviors of the two branches.

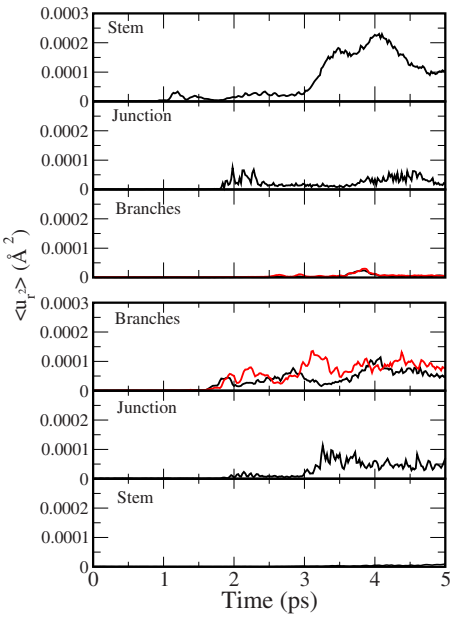


FIG. 6. (Color online) Time evolution of the radial vibrational amplitude during a heat-pulse propagation in the (14,0)-(7,0)-(7,0) Y junction in the forward (upper panel) and backward (lower panel) directions. Black and red (dark gray) lines show the different behaviors of the two branches. The amplitudes show significant reflection and absorption at the junction equally in the forward and reverse directions. Furthermore, the amplitude of the net transmitted radial modes is significantly reduced in both the forward and reverse directions of propagation, indicating that the pulse transport via the radial components is isotropic in nature.

ted radial modes is significantly reduced in both the forward and reverse directions of propagation, and the pulse transport via the radial and azimuthal components is, therefore, isotropic in nature. Vibrational amplitudes corresponding to azimuthal direction were computed and analyzed similarly to the radial and longitudinal amplitudes shown in Fig. 6 and show similar absorption and transmission as seen for radial amplitude in Fig. 6. The anisotropy is thus clearly exhibited only for the longitudinal modes and not for the radial and azimuthal modes.

The simulations were repeated for an armchair (10,10)-(5,5)-(5,5) Y junction (Fig. 1). The initiated thermal pulse is able to traverse the junction in the forward *and* reverse directions with almost equal ease, i.e., no anisotropy was observed during the heat-pulse transport. The contrast between this and the (14,0)-(7,0)-(7,0) Y junction is illustrated in Table I where the values of the three coefficients $T$, $A$, and $R$ are given. The results suggest that thermal pulse rectification may depend on the chirality of the stem and branches of the Y junctions. As pointed out earlier, the topological defects in the form of heptagonal rings have different placings with respect to the junction region for the two Y junctions and this could influence the propagation of the heat pulse differently.

TABLE I. Values of the $T$, $A$, and $R$ coefficients (in percentage). Statistical errors are also quoted.

| | $(14,0)\rightarrow(7,0)\times(7,0)$ | | $(10,10)\rightarrow(5,5)\times(5,5)$ | |
|---|---|---|---|---|
| | Direct | Inverse | Direct | Inverse |
| $T$ | $67\pm4$ | $14\pm2$ | $40\pm4$ | $40\pm6$ |
| $A$ | $25\pm2$ | $40\pm4$ | $38\pm3$ | $38\pm4$ |
| $R$ | $8\pm5$ | $46\pm5$ | $22\pm5$ | $22\pm7$ |

In summary, our results show that the transient heat-pulse transport along a symmetric zigzag Y junction is anisotropic in nature, and the anisotropy can be primarily attributed to the thermal transport due to the axial vibrational modes and not due to the radial modes. The observed anisotropy is very similar to the case of electronic transport in symmetric Y junctions, where a dependency on the underlying lattice structure was found. These findings have important implications in the device application of CNTs. By fabricating CNT Y junctions appropriately, heat pulses can be selectively transmitted in a given direction and blocked in other directions. This shows that carbon nanotube Y junctions can be used for designing and fabricating nanoscale phonon or thermal pulse switching and logic devices in the future.

## ACKNOWLEDGMENTS

E.G.N. gratefully acknowledges useful discussions with L. J. Gallego. Part of this work (E.G.N.) was supported by NASA Ames in 2003–4, and (D.S.) is supported by NASA Contract No. NAS2-03144. D.S. thanks G. Deardorff for useful discussions on visualization of results. M.M. gratefully acknowledges support from grants by DOE (Grants No. DE-FG02-00ER45817 and No. DE-FG02-07ER46375) and U.S.-ARO (Contract No. W911NF-05-1-0372).

*eva.noya@gmail.com
†dsrivastava@mail.arc.nasa.gov
‡super250@pop.uky.edu

[1] J. Li, C. Papadopoulos, and J. Xu, Nature (London) **402**, 253 (1999).
[2] B. C. Satishkumar, P. J. Thomas, A. Govindaraj, and C. N. R. Rao, Appl. Phys. Lett. **77**, 2530 (2000).
[3] A. N. Andriotis, M. Menon, D. Srivastava, and L. Chernozatonskii, Phys. Rev. Lett. **87**, 066802 (2001).
[4] A. N. Andriotis, M. Menon, D. Srivastava, and L. Chernozatonskii, Phys. Rev. B **65**, 165416 (2002).
[5] K. Jensen, J. Weldon, H. Garcia, and A. Zettl, Nano Lett. **7**, 3508 (2007).
[6] J. Hone, M. Whitney, C. Piskoti, and A. Zettl, Phys. Rev. B **59**, R2514 (1999).
[7] M. A. Osman and D. Srivastava, Nanotechnology **12**, 21 (2001).
[8] J. Che, T. Cagin, and W. A. Goddard III, Nanotechnology **11**, 65 (2000).
[9] C. W. Chang, D. Okawa, A. Majumdar, and A. Zettl, Science **314**, 1121 (2006).
[10] G. Wu and B. Li, J. Phys.: Condens. Matter **20**, 175211 (2008).
[11] G. Wu and B. Li, Phys. Rev. B **76**, 085424 (2007).
[12] R. Saito, G. Dresselhaus, and M. S. Dresselhaus, Phys. Rev. B **53**, 2044 (1996).
[13] D. W. Brenner, Phys. Rev. B **42**, 9458 (1990).
[14] Note that, although the temperature was computed from the energy equipartition principle, since the system is not in equilibrium, it is not the real temperature of the system. We will, therefore, refer to this quantity as the kinetic temperature.
[15] M. P. Allen and T. J. Tildesley, *Computer Simulation of Liquids* (Oxford Univeristy Press, New York, 1990).
[16] A. Cummings, M. Osman, D. Srivastava, and M. Menon, Phys. Rev. B **70**, 115405 (2004).